
This is an electronic reprint of the original article.
This reprint may differ from the original in pagination and typographic detail.

Groth, M.; McLean, A. G.; Meyer, W. H.; Leonard, A. W.; Allen, S. L.; Corrigan, G.; Fenstermacher, M. E.; Harting, D.; Lasnier, C. J.; Scotti, F.; Wang, H. Q.; Watkins, J. G.; the DIII-D team

Validation of EDGDE2D-EIRENE predicted 2D distributions of electron temperature and density against divertor Thomson scattering measurements in the low-field side divertor leg in DIII-D

Published in:
Nuclear Materials and Energy

DOI:
[10.1016/j.nme.2023.101372](https://doi.org/10.1016/j.nme.2023.101372)

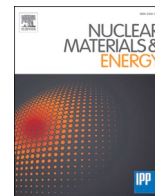
Published: 01/03/2023

Document Version
Publisher's PDF, also known as Version of record

Published under the following license:
CC BY-NC-ND

Please cite the original version:
Groth, M., McLean, A. G., Meyer, W. H., Leonard, A. W., Allen, S. L., Corrigan, G., Fenstermacher, M. E., Harting, D., Lasnier, C. J., Scotti, F., Wang, H. Q., Watkins, J. G., & the DIII-D team (2023). Validation of EDGDE2D-EIRENE predicted 2D distributions of electron temperature and density against divertor Thomson scattering measurements in the low-field side divertor leg in DIII-D. *Nuclear Materials and Energy*, 34, Article 101372. <https://doi.org/10.1016/j.nme.2023.101372>

This material is protected by copyright and other intellectual property rights, and duplication or sale of all or part of any of the repository collections is not permitted, except that material may be duplicated by you for your research use or educational purposes in electronic or print form. You must obtain permission for any other use. Electronic or print copies may not be offered, whether for sale or otherwise to anyone who is not an authorised user.



Validation of EDGDE2D-EIRENE predicted 2D distributions of electron temperature and density against divertor Thomson scattering measurements in the low-field side divertor leg in DIII-D

M. Groth^{a,*}, A.G. McLean^b, W.H. Meyer^b, A.W. Leonard^c, S.L. Allen^b, G. Corrigan^d, M.E. Fenstermacher^b, D. Harting^{d,e}, C.J. Lasnier^b, F. Scotti^b, H.Q. Wang^c, J.G. Watkins^{f,*}, the DIII-D team

^a Aalto University, Espoo, Finland

^b Lawrence Livermore National Laboratory, Livermore, CA, USA

^c General Atomics, San Diego, CA, USA

^d Culham Centre for Fusion Energy, Culham Science Centre, Abingdon, UK

^e Forschungszentrum Jülich, Institute for Energy and Climate Research Plasma Physics, Jülich, Germany

^f Sandia National Laboratory, Albuquerque, NM, USA

ARTICLE INFO

Keywords:

Divertor plasma

DIII-D

Divertor Thomson Scattering

EDGE2D-EIRENE

ABSTRACT

Comparisons of profiles of the electron temperature (T_e), density (n_e) and pressure (p_e) measured with Divertor Thomson Scattering in DIII-D low-confinement mode discharges to predictions from the edge fluid code EDGE2D-EIRENE [1] show that the models implemented in EDGE2D-EIRENE predict the measurements within their collective uncertainties if the T_e at the separatrix ($T_{e,sep}$) is 10 eV, or higher. The simulations do not predict, however, the peaked T_e and n_e profiles measured adjacent to the target plate when $T_{e,sep}$ is below 10 eV, i.e., for the plasma downstream from the region of ionization of deuterium atoms. Inclusion of cross-field drifts and a fivefold reduction of radial transport cannot reconcile the discrepancy between the measurements and predictions.

Introduction

Detachment of the divertor plasma in ITER and in future fusion power plants is one of the primary means to mitigate the otherwise excessive power fluxes to the divertor target plates, and thereby to enable high-performance plasma operation with high duty-cycle of the plant ([2,3] and therein). The onset of detachment is characterized by the reduction of the ion fluxes to the target plates compared to the high-recycling, attached scrape-off layer (SOL) regime, and the formation of a cold (electron temperature, $T_e < 3$ eV) and dense (electron density, $n_e > 1 \times 10^{20} \text{ m}^{-3}$) plasma region adjacent to the target plates. In current tokamaks, detached plasmas are typically achieved when operating at high core plasma, thus SOL densities, close to the density limit. Conceptually, in detached conditions the plasma loses its power volumetrically due to line radiation and Bremsstrahlung, and its momentum due to ion-molecule and ion-atom interaction, and volume recombination. The power fluxes to the target plates in detached conditions are

determined by the surface recombination of plasma particles to molecules due to remaining plasma (fluxes) to the target plates and radiative heating. For reactor-relevant conditions, a residual fuel ion flux of $1 \times 10^{24} \text{ m}^{-2} \text{ s}^{-1}$ at 2 eV results in 5 MW/m^2 , highlighting the need for significant reduction of the fuel ion fluxes and thus high degree of detachment. Understanding and being able to predict the onset and formation of divertor plasma detachment is one of the most critical tasks in magnetic confinement fusion.

Reproducing the measured plasma and neutral conditions obtained in today's tokamaks with currently the most complete edge fluid codes has been shown to be challenging, even for low-confinement (L-mode) plasmas exhibiting significantly shallower radial and poloidal gradients and no Edge-Localized Modes (ELMs) compared to high-confinement mode (H-mode) plasmas: SOLPS5.0 and SOLPS-ITER for ASDEX Upgrade [4,5] and DIII-D [6], EDGE2D-EIRENE for JET [7,8] and UEDGE for DIII-D [9] consistently underestimate the ion fluxes to the low-field side (LFS) target plate in high-recycling conditions. The code predictions

* Corresponding authors at: Aalto University, Otakaari 1, 02150 Espoo, Finland.

E-mail address: mathias.groth@aalto.fi (M. Groth).

<https://doi.org/10.1016/j.nme.2023.101372>

Received 12 June 2022; Received in revised form 23 December 2022; Accepted 19 January 2023

Available online 25 January 2023

2352-1791/© 2023 The Author(s). Published by Elsevier Ltd. This is an open access article under the CC BY-NC-ND license (<http://creativecommons.org/licenses/by-nc-nd/4.0/>).

are generally in agreement with the measurements in low-recycling conditions.

To further elucidate the validity of the predicted SOL conditions in DIII-D L-mode plasmas using EDGE2D-EIRENE [10], the simulations are post-processed for T_e , n_e and the electron pressure (p_e) across the LFS

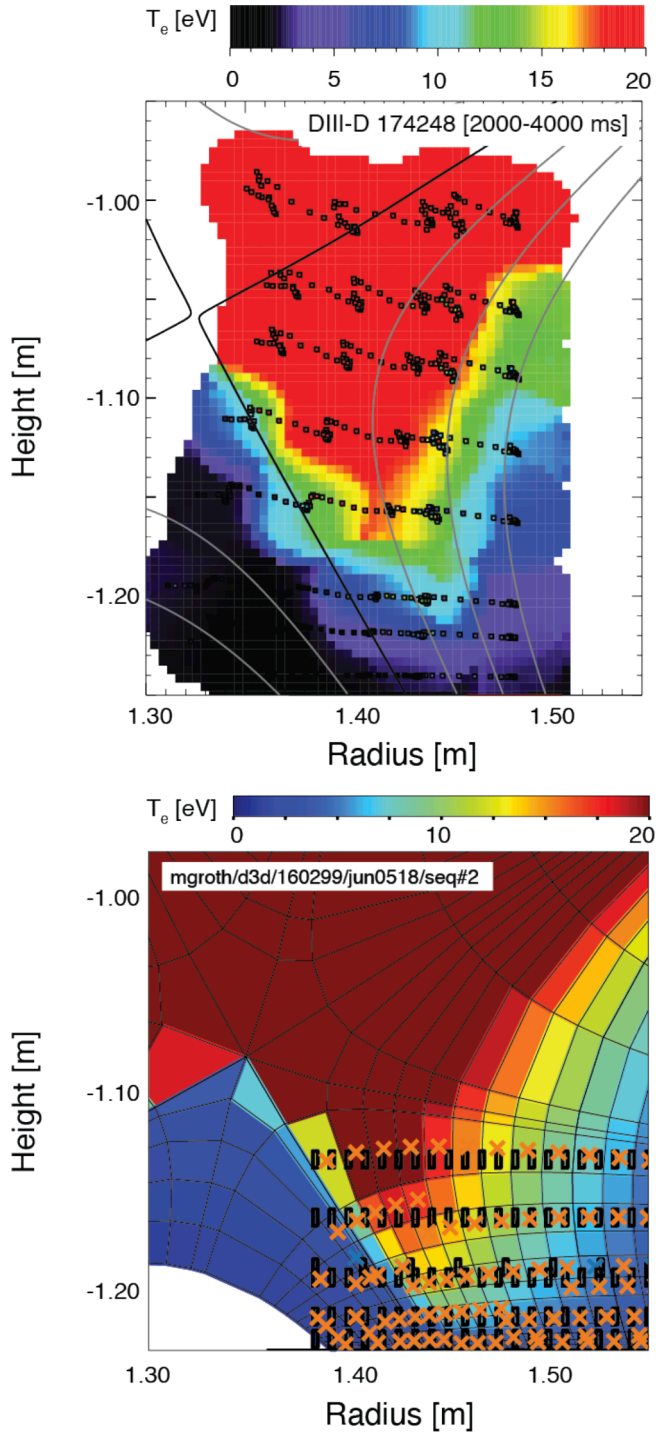


Fig. 1. (a) 2D color contour plot of T_e in a high-recycling, low-confinement mode plasmas (DIII-D 174248) inferred from a 20 cm strike point sweep across the DTS photon scattering points and mapped to a single magnetic equilibrium (DIII-D 174,248 at 2200 ms). The actual DTS data points are indicated by the black squares. (b) 2D color contour plot of the EDGE2D-EIRENE predicted T_e (case: mgroth/d3d/160299/jun0518/seq#2). The assumed DTS photon scattering points are shown as crosses for the nearest cell neighbor and squares for the surface-averaged assumption using the actual DTS collection areas.

divertor plasmas using the measurement locations of the Divertor Thomson Scattering (DTS) system (Fig. 1) [11,12]. Here, the 2D DTS data, obtained by sweeping the LFS strike point across the lower divertor target, were rearranged as radial, approximately horizontal profiles per vertical channel for the five lowermost channels. In previous studies [10], the most significant discrepancies between the measured and EDGE2D-EIRENE predicted profiles were obtained in high-recycling conditions, for which the measured T_e and n_e profiles across the lowermost DTS channel were more peaked outboard of the separatrix, and n_e a factor of 2–3 higher than predicted (Ref. [10] Fig. 5a and b). The previous studies also showed agreement for T_e and n_e within 20 % between the DTS measurements and EDGE2D-EIRENE predictions for low-recycling conditions (Ref. [10], Fig. 1b and c). To further elaborate on this agreement, and to isolate the region of disagreement to the area below the ionization region of deuterium atoms in high-recycling and detached conditions, the analyses in this report are also carried out for low-recycling conditions.

Description of discharges, DTS data analyses and EDGE2D-EIRENE setup

Low-recycling, intermediate-recycling, high-recycling and partially detached divertor plasma conditions at the LFS divertor target were established by varying the core plasma density through deuterium injection into the DIII-D main chamber. These plasmas were heated with approximately 0.9–1.1 MW of ohmic heating power, supplemented with 10-ms neutral beam blips of a 10 % duty cycle for charge-exchange ion-temperature (T_i) measurements. The plasma current was 1.1 MA, the toroidal field 2.1 T, with the ion $B \times \nabla B$ drift direction into the lower divertor. The lower single null magnetic equilibrium and the divertor geometry were as shown in Ref. [11], Fig. 1. The plasma-facing components in DIII-D are ATJ graphite, hence, carbon is the primary plasma impurity species (of approx. concentration 1 % just inboard of the separatrix at the LFS midplane). The discharges were repeated up to six times for spectroscopy purpose, which resulted in improved statistics of the DTS data. The DTS data were accumulated over these discharges and mapped onto the magnetic equilibrium calculated by EFIT [13] as the distance from the separatrix measured at the LFS midplane ($R-R_{sep,LFS-mp}$) for each vertical channel.

Beside the ambiguity of the radial position of the separatrix in the main and divertor SOL, further uncertainty is the measurements is introduced by the 20 cm strike point sweep to reconstruct the 2D profile on T_e , n_e and p_e in the divertor. During the strike point sweep the line-averaged density measured at the LFS midplane was held constant within 5 % of the mean value, and the D_2 pressure in the lower sub-divertor did not change, indicating that the neutral conditions in the divertor were not affected by the sweep. However, during the strike point sweep, the X-point height was lower by 2 cm, resulting in a 10 % reduction of the poloidal distance from the X-point to the LFS strike point (approximately 2.5 cm out of 22 cm). The ion saturation current to the LFS target plate, inferred from an array of radially spaced Langmuir probe covering the LFS plate, was measured continuous with no indication of changes to the current densities during the sweep (Fig. 5c in [10]). Similar, the line-integrated radial Lyman- α and Balmer- α emission profiles (Fig. 5a and b in [10]), obtained during the sweep, do not show any significant changes in the deuterium emission profiles that would suggest significant changes in the plasma conditions. These observations are corroborated by combining DTS data from D_2 fueling ramps with fixed strike point positions – obtained in configurations for which the DTS chords were aligned with the LFS strike point and the divertor X-point, respectively – with data from strike point sweeps at constant core plasma density. For the same line-averaged density at the LFS midplane during the fueling ramp, and the same $R-R_{sep,LFS-mp}$, T_e , n_e and p_e are measured the same as during the sweeps. For high-recycling conditions, imaging of the C III (465 nm) emission, however, showed the peak emission during the sweep to move from the LFS X-point to the LFS

strike point region, along a continuous band of C III emission tracking the LFS divertor separatrix. It is unclear whether the spatial change of C III emission is due to increased carbon density or changes in T_e and n_e . As the sweep potentially deliberates (co-deposited) carbon as the sweep progresses toward larger major radius, it is conceivable that the C^{2+} density increased locally, while the reduction in X-point height increases the T_e and n_e at the LFS strike point. These changes in the emission profiles indicate the general sensitivity of the measurements on both parameters. Lastly, changes to the SOL flow pattern in the LFS divertor leg due to reduction in X-point height are also conceivable, but these measurements do not exist for these plasmas.

The EDGE2D-EIRENE code package [1,14,15] with preset-power and zero-particle flux conditions at the core boundary, and an assumed, purely diffusive radial transport model was adapted to the measured SOL conditions at the LFS midplane. The SOL conditions in both the HFS and LFS divertor legs are the primary output of the simulations. The code setup was described in Ref. [10], and the identical setup was used for this report, including the variations in the power imposed at the assumed core boundary ($P_{\text{core-bd}}$) capturing the uncertainties in radiated power inside the core plasma: 0.9 MW for the low-recycling case (n_e at the LFS midplane, $n_{e,\text{sep,LFS-mp}}$, of $0.8 \times 10^{19} \text{ m}^{-3}$) and 1.2 MW for the high-recycling case ($n_{e,\text{sep,LFS-mp}}$ of $2.0 \times 10^{19} \text{ m}^{-3}$). The radial profiles of T_e , T_i and n_e were determined by $P_{\text{core-bd}}$, $n_{e,\text{sep,LFS-mp}}$ and the choices of radially dependent transport coefficients for ions (D_{\perp}), and electron and ion heat (χ_e and χ_i , respectively.) The transport coefficients were determined manually and iteratively using the measured profiles using the core Thomson scattering system (Fig. 2). Here, a transport barrier across the separatrix was imposed by reducing D_{\perp} from $0.5 \text{ m}^2/\text{s}$ to $0.25 \text{ m}^2/\text{s}$ inside the separatrix, corresponding to the n_e pedestal region, and raised exponentially to $4.5 \text{ m}^2/\text{s}$ to obtain the measured fall-off of n_e across the SOL (approximately 5 cm). Similarly, to reproduce the measured T_e profile at the LFS midplane, including T_e at the separatrix ($T_{e,\text{sep,LFS-mp}}$), χ_e was raised from $1 \text{ m}^2/\text{s}$ in the core region to $2 \text{ m}^2/\text{s}$ in the SOL, while a constant χ_i of $0.75 \text{ m}^2/\text{s}$ in both the core and SOL regions were assumed. Below the X-point, spatially constant diffusivities (initially, $D_{\perp} = \chi_e = 1 \text{ m}^2/\text{s}$, $\chi_i = 0.75 \text{ m}^2/\text{s}$) were assumed. In these studies, the same profiles and values of the transport coefficients are

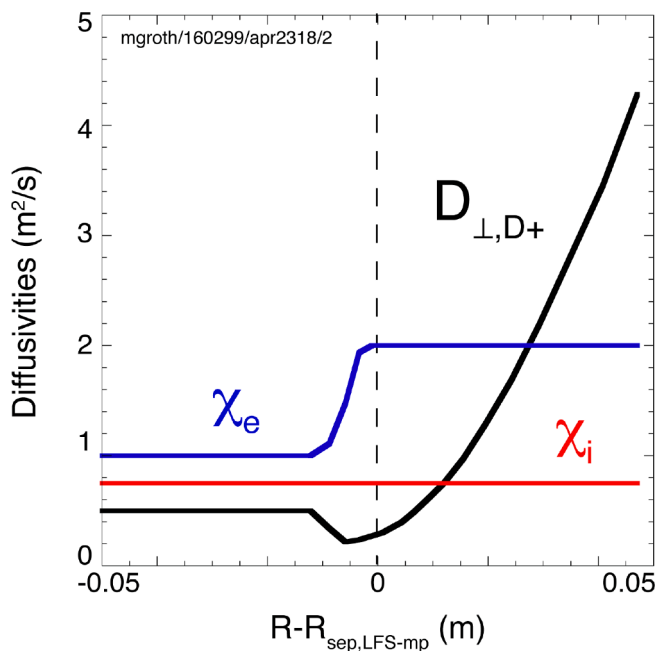


Fig. 2. Radial profiles of the assumed diffusive transport coefficients in the main SOL in EDGE2D-EIRENE simulations pertaining to both low-recycling and high-recycling conditions: ion particle diffusion coefficient D_{\perp} (black), electron heat coefficient, χ_e (blue) and ion heat coefficient, χ_i (red).

assumed for both low-recycling and high-recycling conditions. At the core boundary, the inward going atomic flux is negligible, and the inward and outward going ion currents are balanced. The walls, including the divertor targets, are assumed to be fully saturated with deuterium, hence particle recycling coefficients of unity were assumed both for the deuterons, and deuterium atoms and molecules. In the code runs $n_{e,\text{sep,LFS-mp}}$ is preset and controlled by D_2 gas injection from a location in the main chamber representing the actual DIII-D gas injection system, and pumping below the divertor shelf approximating the DIII-D cryogenic pump geometry in the lower divertor. To address the uncertainties of plasma conditions at separatrix, thus the location of the separatrix, $P_{\text{core-bd}}$ and $n_{e,\text{sep,LFS-mp}}$ were varied systematically by 10–20 % to lower and higher values. Experimentally, $T_{e,\text{sep,LFS-mp}}$, and thus $n_{e,\text{sep,LFS-mp}}$, were inferred from power balance for the SOL assumed in the conduction-limited regime [16]. As in Ref. [10], the reaction rates for plasma-atomic and plasma-molecular processes were identical to those published in [17], carbon was included in the simulations as the primary impurity species, and cross-field drifts and currents were invoked on the plasma species. The cross-field drifts include radial drifts due to the poloidal electric field and the poloidal drifts due to the radial electric field, and thermo-electric currents due to the finite resistivity of the SOL plasma [18].

To address the finite photon collection volume of the DTS system (0.5 cm wide and 1.3 cm tall), which often cuts through several EDGE2D-EIRENE grid cells in areas of strong grid cell compressions (e. g., at the separatrix), the EDGE2D-EIRENE data was surface-averaged over the assumed DTS spatial points (Fig. 1b). This analysis technique produced smoother radial profiles of the predicted plasma parameters, but sampling the nearest neighboring cells to the center of the assumed DTS point produced nearly identical results. Hence, radial and horizontal averaging is excluded as a potential root cause for the previously reported discrepancy between measurements and predictions.

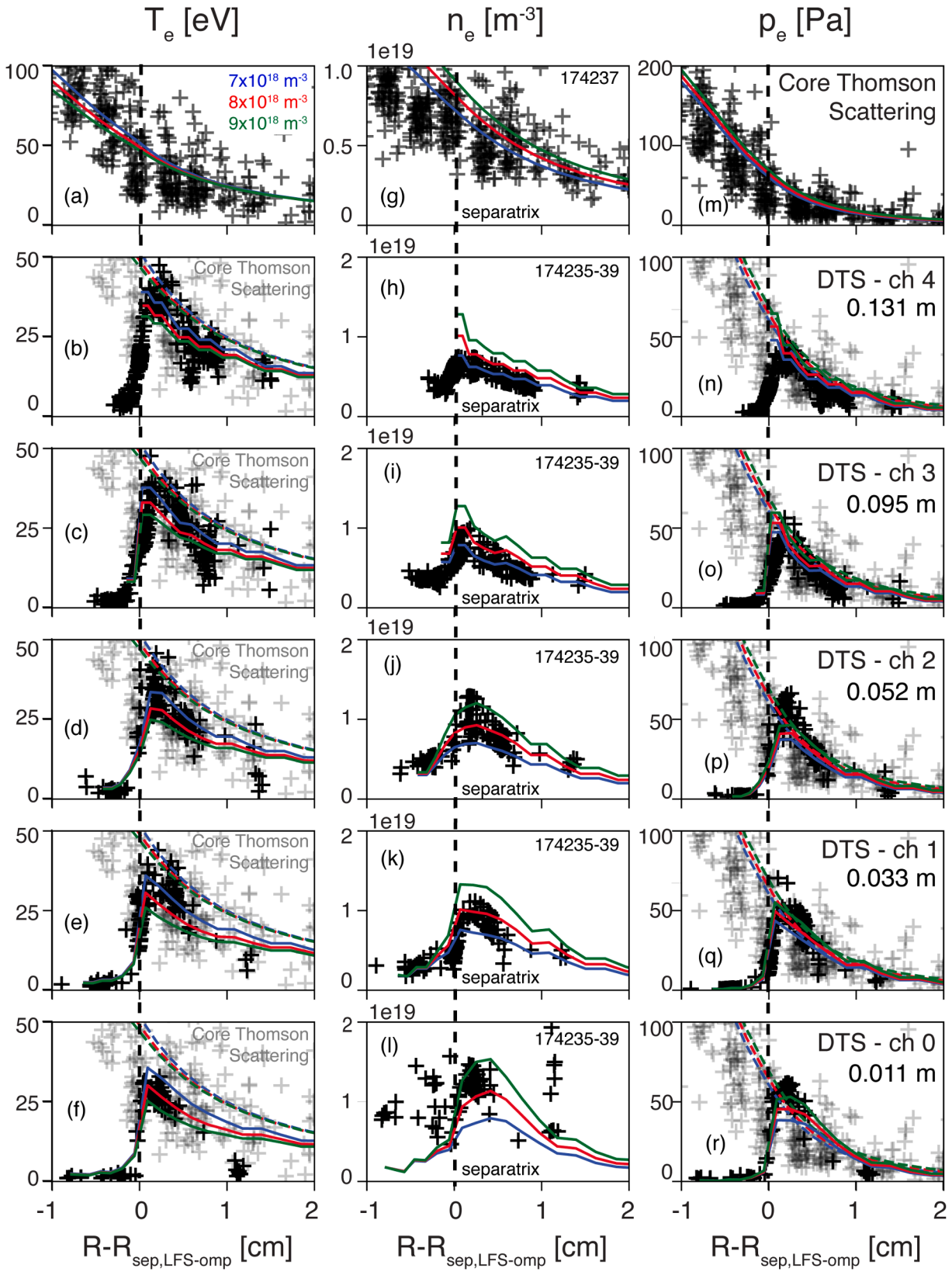
Comparison of EDGE2D-EIRENE predicted plasmas conditions to DTS in low-recycling conditions

In the simulations of the low-recycling conditions, assuming $n_{e,\text{sep,LFS-mp}}$ of $8 \times 10^{18} \text{ m}^{-3}$ and $P_{\text{core-bd}}$ of 0.9 MW reproduced the peak T_e , n_e and p_e for all DTS channels within 20 % of the measured values, while lowering and raising $n_{e,\text{sep,LFS-mp}}$ by $1 \times 10^{18} \text{ m}^{-3}$ exact matches to individual DTS radial profiles can be obtained (Fig. 3). The predicted values of $T_{e,\text{sep,LFS-mp}}$ (44–46 eV) is lower than the experimentally inferred value at the LFS-midplane (approximately 50 eV), but well within the uncertainty of the measurements. Previously, for identical L-mode plasmas, $T_{e,\text{sep,LFS-mp}}$ was measured to be 40–50 eV with Thomson Scattering and the reciprocating probe (Fig. 2b in Ref. [19]). Furthermore, the measured profiles indicated a steeper slope inside and outside the separatrix than the predicted ones (Fig. 3a, predictions consistently above the center of gravity of the Thomson Scattering measurements), calling into question the current choices of the radial transport coefficients and indicate their further refinement. Consequently, the predicted radial profiles of T_e in the LFS divertor plasma are consistently broader by a factor of 2 than the measured profiles (Fig. 3b-f).

The sensitivity of n_e across the LFS divertor on the assumed $n_{e,\text{sep,LFS-mp}}$ is strong: while the lower bound of $n_{e,\text{sep,LFS-mp}}$ reproduces the DTS profiles near the X-point fairly accurately (Fig. 3h,i), the upper bound of $n_{e,\text{sep,LFS-mp}}$ is required to reproduce DTS profiles near the divertor plate (Fig. 3k,l). For the lowermost DTS channel the difference in the peak n_e between the upper and lower bound cases is approximately a factor of 2, highlighting the anticipated sensitivity of the divertor plate conditions on $n_{e,\text{sep,LFS-mp}}$.

A lesser sensitivity of the plasma conditions at the LFS target plate was observed when systematically varying $T_{e,\text{sep,LFS-mp}}$ via the assumed power across the simulation grid core boundary by 100 kW out of 900 kW (not shown).

Both the measurements and the simulations suggest that in these



[mgroth/d3d/160299/apr2318/1](https://doi.org/10.1016/j.nme.2023.101372) [mgroth/d3d/160299/apr2318/2](https://doi.org/10.1016/j.nme.2023.101372) [mgroth/d3d/160299/apr2318/3](https://doi.org/10.1016/j.nme.2023.101372)

Fig. 3. Radial profiles of the measured and EDGE2D-EIRENE predicted T_e (a-f), n_e (g-l) and p_e (m-r) for DIII-D low-density discharges 174235-39 in the low-recycling regime. The profiles are ordered by rows for the LFS midplane (a, g, m; DIII-D 174237 only) and DTS channels 4 through 0 from the LFS X-point region to the LFS target plate. EDGE2D-EIRENE simulations assuming $P_{\text{core-bd}} = 0.9$ MW and $n_{e,\text{sep,LFS-mp}} = 7 \times 10^{18} \text{ m}^{-3}$ (blue), $8 \times 10^{18} \text{ m}^{-3}$ (red) and $9 \times 10^{18} \text{ m}^{-3}$ (green) are post-processed for the DTS geometry as shown in Fig. 1. The measured and predicted LFS midplane profiles for T_e and p_e are repeated for each DTS row and are shown as grey crosses and dashed lines, respectively. The poloidal distance of each DTS channel to the LFS plate at the separatrix is given in (h) through (l). The poloidal distance from the X-point to the LFS plate is 0.2 m. All profiles are presented as distance from the separatrix ($R - R_{\text{sep,LFS-omp}}$). The separatrix is shown as the black vertical dashed line.

low-recycling conditions p_e is conserved in the parallel-B direction of the SOL consistent with analytic models, e.g., two-point model [20]. Since the T_e gradients in the poloidal direction are weak, simulations without cross-field drifts and thermo-electric currents are similar to those with the drifts included (Fig. 4). However, the simulations with the cross-field drifts and thermo-electric currents included predict strong flow from the LFS to the HFS plate in the private flux region, as observed experimentally and in previous edge fluid simulations (e.g., [9] for UEDGE).

Comparison of EDGE2D-EIRENE predicted plasmas conditions to DTS in high-recycling conditions

For high-recycling SOL conditions EDGE2D-EIRENE indicates a stronger dependence of the divertor conditions on $T_{e,sep,LFS-mp}$ (32 eV for an assumed 0.9 MW across the core boundary, versus 39 eV for 1.2 MW and 44 eV for 1.4 MW, Fig. 5) and a weaker dependence on $n_{e,sep,LFS-mp}$ ($1.8 \times 10^{19} \text{ m}^{-3}$ versus $2.0 \times 10^{19} \text{ m}^{-3}$ and $2.2 \times 10^{19} \text{ m}^{-3}$, not shown). The experimentally inferred T_e profiles at the LFS midplane suggest $T_{e,sep,LFS-mp}$ to be between 40 eV and 50 eV, consistent with previous measurements of $T_{e,sep,LFS-mp}$ (50 eV, Fig. 5b in Ref. [19]) in similar plasmas. Consequently, when imposing $T_{e,sep,LFS-mp}$ of 40 eV, EDGE2D-EIRENE predicts the peak T_e (Fig. 5b-e) and n_e (Fig. 5h-k) for all DTS channels with the exception of the lowermost DTS channel (Fig. 5f, 5 l). Specifically, for the lowermost channel the simulations underpredict the measured peak n_e by a factor of 2 (Fig. 5l) and the discrepancy cannot be remedied when increasing $n_{e,sep,LFS-mp}$ to $2.2 \times 10^{19} \text{ m}^{-3}$, and beyond (not shown, for peak n_e , see Fig. 1b in [10]). The predicted peak n_e at the uppermost DTS channel (Fig. 5h) is 50 % higher than measured likely due to the coarse grid describing the X-point region; its resolution requires grids with higher spatial resolution.

While the predicted T_e and n_e profiles for the uppermost DTS channels are as broad as suggested by the DTS measurements (Fig. 5b-d, 5 h-j), they are consistently broader for the two lowermost channels (Fig. 5e-f, 5 k-l). Across the lowermost channel the predicted T_e profiles peak in the mid SOL, while the DTS measurements showed the peak T_e approximately 1 cm (in $R-R_{sep,LFS-mp}$ space) radially outboard of the EFIT predicted outer strike point location (Fig. 5f). Similarly, the measured n_e profile peaked at the LFS strike point, while in the simulations the peak is 2 mm radially outboard from the LFS strike point (Fig. 5l).

Both the measured and the EDGE2D-EIRENE predicted p_e indicate loss of plasma pressure, thus momentum, between the LFS midplane and the lowermost DTS channel, and therefore show pressure losses already at the onset of detachment: the p_e profiles across the lowermost DTS channel are reduced by approximately 1/2 compared to the p_e profiles at the LFS midplane (Fig. 5r). This observation is valid for the measured p_e (grey versus black crosses) and the EDGE2D-EIRENE predictions (dashed-colored lines versus solid-colored lines). The radial profiles of p_e exhibit the same discrepancy in the peak location as the n_e profiles.

Omitting cross-field drifts and currents from the simulations predicts the n_e profiles across the two lowermost DTS channels to peak approximately 3 mm (in $R-R_{sep,LFS-mp}$ space) further radially outward than in simulations including the drifts (Fig. 6). Such change in the predicted density profiles is consistent with poloidal T_e gradients across the lowermost DTS channels (Fig. 6l) driving radial ion flow due to ExB drifts (poloidal electric field crossed with B_T) toward the separatrix in this B_T configuration. Compared to the poloidal and radial T_e gradients observed in H-mode plasmas, and thus cross-field drifts (e.g., [21]), the impact of radial drifts is rather benign in these L-mode plasmas.

Discussion

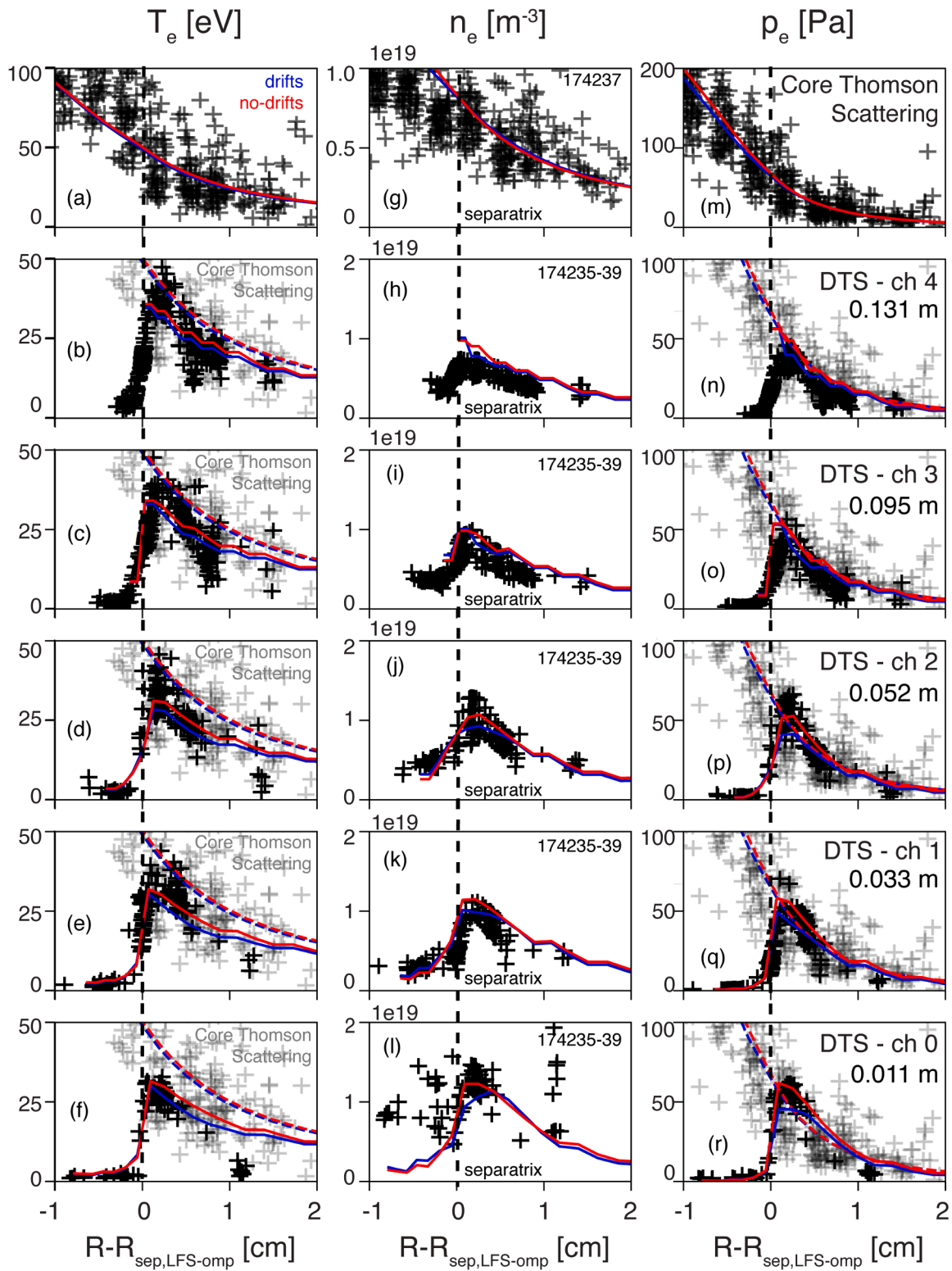
The comparison of DTS measurements and EDGE2D-EIRENE predictions of T_e , n_e and p_e across the LFS divertor highlights the validity of the Bragiński transport model in the parallel-B direction in the SOL when $T_{e,sep}$ in the SOL is above 10 eV, i.e., when the ionization region of deuterium atoms is adjacent to the divertor plate. Conversely, the

comparisons indicate an increasing deviation between the measurements and the prediction for the SOL region downstream from the ionization front in high-recycling conditions. The threshold value of 8–10 eV is further constrained by an intermediate density case (at $n_{e,sep,LFS-mp}$ to $1.4 \times 10^{19} \text{ m}^{-3}$, see Fig. 1 in reference [10]) for which EDGE2D-EIRENE predicts for the lowermost DTS channel the peak value of T_e and the profile of n_e , including the peak value, while broader T_e profiles than measured. Significantly stronger disagreement is therefore anticipated for partially and fully detached conditions (see Ref [10], Fig. 1a and b). In all EDGE2D-EIRENE simulations conducted thus far, the predicted T_e and n_e profiles adjacent to the LFS target plate are significantly shallower than the measured T_e and n_e profiles, indicating a shortcoming in either, or the sum of, the poloidal transport model, the radial transport model, the applied boundary conditions at the LFS plate, or yet unaccounted physics, such as additional plasma ion–molecule interaction and plasma redistribution due to photon opacity. Cross-field drifts and thermo-electric currents are predicted to play a minor role in the plasma distribution in the LFS leg in these conditions. In the high-density region of the lowermost DTS channel, T_e is between 2 and 3 eV, and not at or below 1 eV, hence, three-body volume recombination is not expected to play a role in determining the radial position and height of n_e peak. The measurements are highly reproducible in a series of 5–7 identical discharges, and thus currently not considered the source of the deviation. The T_e measurements indicated larger scatter in the region 2–4 mm radial outboard of the LFS strike point, for T_e of approximately 2–4 eV, which might be indicative of a fluctuating plasma in these conditions, or a diagnostic issue. The uncertainties in the DTS measurements due to the divertor strike point sweep appear to be of lesser significance than the EDGE2D-EIRENE model assumptions.

In these studies, identical diffusivities for ion (D_{\perp}) and heat (χ_e, χ_i) were applied for both the low-recycling and high-recycling SOL conditions: the measured profiles of T_e and n_e at the LFS midplane were reproduced within the uncertainties of the measurements, including the position of the separatrix, by setting $n_{e,sep,LFS-mp}$ by D_2 gas injection and pumping, and $T_{e,sep,LFS-mp}$ by the power across the code core surface. Further improvements of constraining the prescribed profiles can be made by choosing different sets of D_{\perp} , χ_e , and χ_i . However, these studies reproduce the strong sensitivity of the divertor SOL conditions on the prescribed $n_{e,sep,LFS-mp}$ and $T_{e,sep,LFS-mp}$, which was observed in previous simulations, also by other authors, which cannot be resolved by any closer approximation of the measured profiles at the LFS midplane.

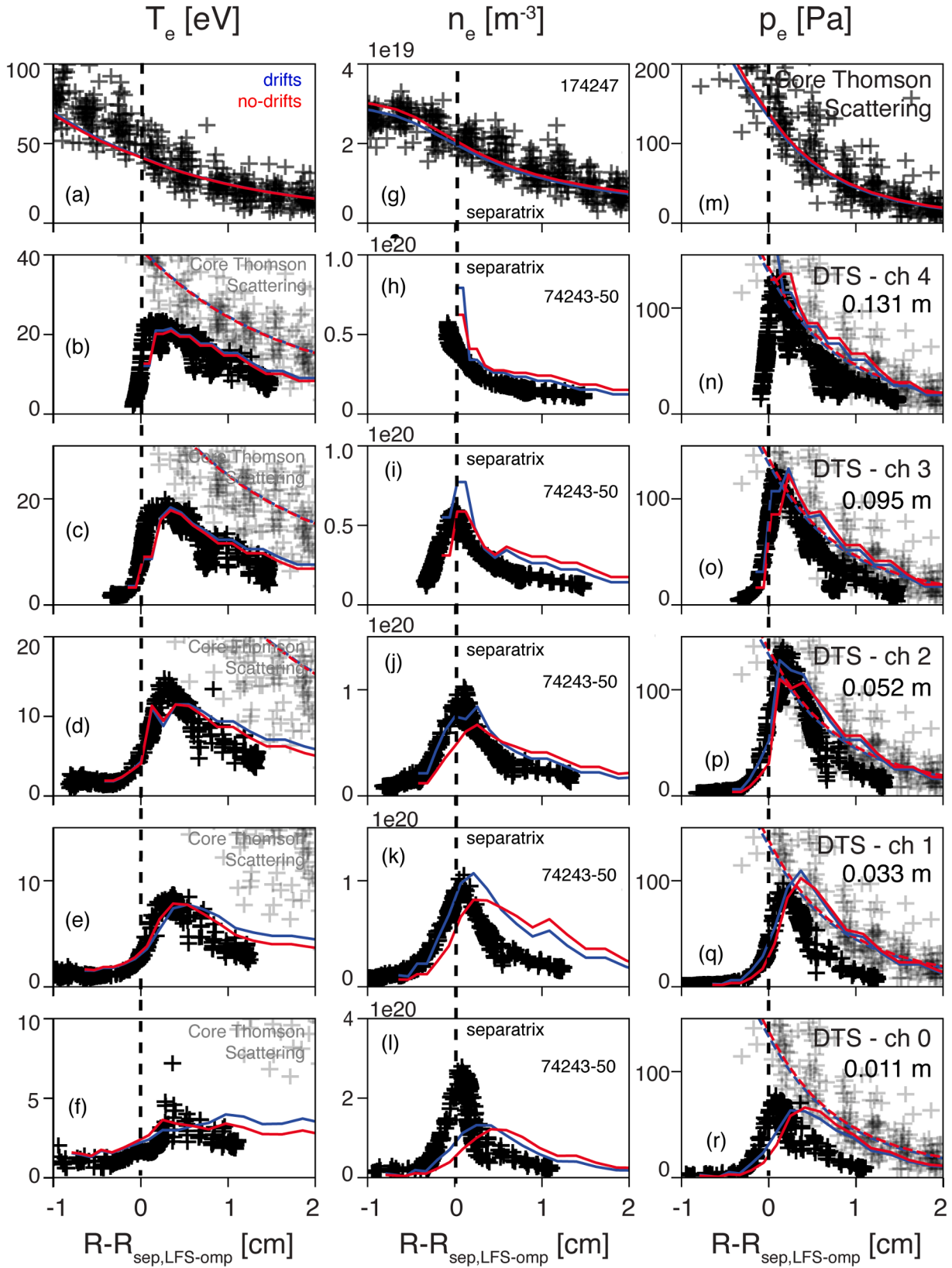
Reducing radial transport in the divertor plasma by decreasing the radial diffusivities for ion (D_{\perp}) and electron heat transport (χ_e) by factors of 5 and 10, respectively, while maintaining the same D_{\perp} and χ_e in the main SOL, resulted in neither a shift of the n_e peak toward the separatrix nor and a peaking of T_e profiles across the lowermost DTS channel. The reduction in D_{\perp} , however, made the predicted DTS profiles upstream of the ionization front more peaked for n_e , but broader for T_e . Reducing χ_e had no impact on either the predicted n_e and T_e profiles. The application of poloidally and radially varying transport coefficients in the LFS divertor leg, and the introduction of convective radial transport via prescribed radial velocities has not yet been attempted. Secondly, lowering χ_e in the main SOL resulted in steeper T_e profiles at the LFS midplane, and thus in the uppermost divertor DTS channels. However, by doing so $T_{e,sep,LFS-mp}$ was also reduced, from 39 eV to 37 eV, which cause the predicted peak T_e across all DTS channels to decrease by a factor of two, causing further disagreement between the predictions and the measurements. These results indicate the sensitivity of predicted divertor conditions on $T_{e,sep,LFS-mp}$ (and $n_{e,sep,LFS-mp}$), the lack of an adequate radial transport model, and highlight the need for accurate measurements of the separatrix location at the LFS midplane.

For both low-recycling and high-recycling conditions EDGE2D-EIRENE reproduced the measured Lyman and Balmer across the LFS divertor leg [10,22]. However, the simulations did not reproduce the C IV emission in high-recycling conditions, which is likely also related to underpredicting the n_e profile across the lowermost DTS channel [22].



mgroth@3sd/160299/apr2318/2 mgroth@3sd/160299/mar0518/4

Fig. 4. Radial profiles of the measured and EDGE2D-EIRENE predicted T_e (a-f), n_e (g-l) and p_e (m-r) for DIII-D low-density discharges 174235–39 in the low-recycling regime. The profiles are ordered by rows for the LFS midplane (a, g, m; DIII-D 174237 only) and DTS channels 4 through 0 from the LFS X-point region to the LFS target plate. EDGE2D-EIRENE simulations assuming $P_{\text{core-bd}} = 0.9$ MW and $n_{e,\text{sep,LFS-mp}} = 8 \times 10^{18} \text{ m}^{-3}$ including (blue) and excluding cross-field drifts (red) are post-processed for the DTS geometry as shown in Fig. 1. The measured and predicted LFS midplane profiles for T_e and p_e are repeated for each DTS row and are shown as grey crosses and dashed lines, respectively. The poloidal distance of each DTS channel to the LFS plate at the separatrix is given in (h) through (l). The poloidal distance from the X-point to the LFS plate is 0.2 m. All profiles are presented as distance from the separatrix ($R-R_{\text{sep,LFS-mp}}$). The separatrix is shown as the black vertical dashed line.



mgroth/d3d/160299/jun0518/2 mgroth/d3d/160299/apr1619/5

Fig. 6. Radial profiles of the measured and EDGE2D-EIRENE predicted T_e (a-f), n_e (g-l) and p_e (m-r) for DIII-D low-density discharges 1742443–50 in the high-recycling regime. The profiles are ordered by rows for the LFS midplane (a, g, m; DIII-D 174247 only) and DTS channels 4 through 0 from the LFS X-point region to the LFS target plate. EDGE2D-EIRENE simulations assuming $P_{core-bd} = 1.2$ MW and $n_{e,sep,LFS-mp} = 2.0 \times 10^{19} m^{-3}$ including (blue) and excluding cross-field drifts (red) are post-processed for the DTS geometry as shown in Fig. 1. The measured and predicted LFS midplane profiles for T_e and p_e are repeated for each DTS row and are shown as grey crosses and dashed lines, respectively. The poloidal distance of each DTS channel to the LFS plate at the separatrix is given in (h) through (l). The poloidal distance from the X-point to the LFS plate is 0.2 m. All profiles are presented as distance from the separatrix ($R - R_{sep,LFS-mp}$). The separatrix is shown as the black vertical dashed line.

The agreement between the measured and predicted Lyman- α and Balmer- α emission in high-recycling conditions reiterate that the origin of these emissions is within the ionization front and electron-excitation driven, as shown in Ref. [10].

While for the same plasmas in the high-recycling regime the edge fluid code UEDGE [23] indicates the same factor-of-2 underprediction of the peak n_e at the LFS plate, UEDGE predicts the T_e profile, including the peak T_e of 4–5 eV as measured [24], indicating the need to further investigations of the root cause for the observed discrepancies between the measurements and EDGE2D-EIRENE.

Summary

In this report the previously reported disagreement between EDGE2D-EIRENE predictions and measurements of the plasma conditions in high-recycling conditions at the LFS divertor plate in DIII-D L-mode plasmas [10] was isolated to the region downstream from the ionization of deuterium atoms ($T_{e,sep} < 10$ eV). The simulations show that the profiles of T_e , n_e and p_e across five radial channels of the DTS are predicted within the uncertainties of the LFS midplane and DTS measurements, and the code setup, if $T_{e,sep}$ remains above 10 eV along the SOL and thus the ionization of deuterium to occur at the LFS plate. These observations are consistent with previous simulations of DIII-D, ASDEX Upgrade and JET. Thus far, EDGE2D-EIRENE simulations do not predict the plasma in the region downstream from the primary ionization of deuterium, for which the predicted peak n_e is a factor of 2 too low and to peak radially outboard from the measured peak, and the profiles of T_e significantly flatter than measured. Reducing radial transport in the divertor by factors of 5 for particles and 10 for electron heat did not result in significant improvements of the experiment-code agreement. Cross-field drifts and thermo-electric currents are predicted to play a minor role in the plasma distribution in the LFS leg in both low-recycling and high-recycling conditions.

Disclaimers

This report was prepared as an account of work sponsored by an agency of the United States Government. Neither the United States Government nor any agency thereof, nor any of their employees, makes any warranty, express or implied, or assumes any legal liability or responsibility for the accuracy, completeness, or usefulness of any information, apparatus, product, or process disclosed, or represents that its use would not infringe privately owned rights. Reference herein to any specific commercial product, process, or service by trade name, trademark, manufacturer, or otherwise, does not necessarily constitute or imply its endorsement, recommendation, or favoring by the United States Government or any agency thereof. The views and opinions of authors expressed herein do not necessarily state or reflect those of the United States Government or any agency thereof.

Declaration of Competing Interest

The authors declare that they have no known competing financial interests or personal relationships that could have appeared to influence the work reported in this paper.

Data availability

Data will be made available on request.

Acknowledgements

This work was supported by US DOE under contract nos. DE-FC02-04ER54698, DE-AC52-07NA27344, DE-AC05-00OR22725 and DE-NA0003525. This work has been carried out within the framework of the EUROfusion Consortium and has received funding from the Euratom research and training programme 2014-2018 and 2019-20 under grant agreement number 633053. The views and opinions expressed herein do not necessarily reflect those of the European Commission. The authors would like to thank Mr. Henri Kumpulainen of Aalto University for his extraordinary and very much appreciated Python scripting support.

References

- [1] S. Wiesen, EDGE2D-EIRENE code interface report, JET ITC-Report, <http://www.eirene.de/e2deir_report_30jun06.pdf>, 2006.
- [2] ITER Physics Expert Group on Divertor et al., Chapter 4: Power and particle control, Nuclear Fusion 39 (1999) 2391.
- [3] A. Loarte et al., Chapter 4: Power and particle control, Nuclear Fusion 47 (2007) S203.
- [4] L. Aho-Mantila, et al., Plasma Physics and Controlled Fusion 59 (2017), 035003.
- [5] H. Wu, et al., Plasma Physics and Controlled Fusion 63 (2021), 105005.
- [6] J.M. Canik, et al., Physics of Plasmas 24 (2017), 056116.
- [7] M. Groth, et al., Nuclear Fusion 53 (2013), 093016.
- [8] C. Guillemaut, et al., Nuclear Fusion 54 (2014), 093012.
- [9] M. Groth, et al., Plasma Physics and Controlled Fusion 53 (2011), 124017.
- [10] M. Groth, et al., Nuclear Materials and Energy 19 (2019) 211.
- [11] A.G. McLean, et al., Journal of Nuclear Materials 463 (2015) 533.
- [12] F. Glass, et al., Review Scientific Instruments 87 (2016) 11E508.
- [13] L.L. Lao, et al., Nuclear Fusion 25 (1985) 1611.
- [14] R. Simonini, et al., Contributions to Plasma Physics 34 (1994) 368.
- [15] D. Reiter, et al., Journal of Nuclear Materials 196–198 (1992) 80.
- [16] A.W. Leonard, et al., Nuclear Fusion 57 (2017), 086033.
- [17] V. Kotov, et al., Plasma Physics and Controlled Fusion 50 (2008), 105012.
- [18] R. Zagorski, et al., Modelling of Drifts and Currents in the Edge Plasma, Forschungszentrum Jülich, Germany, report JUEL-3829 (2000).
- [19] D.L. Rudakov, et al., Nuclear Fusion 45 (2005) 1589.
- [20] C.S. Pitcher, et al., Plasma Physics and Controlled Fusion 39 (1997) 779.
- [21] A.E. Jaervinen, et al., Physical Review Letters 121 (2018), 075001.
- [22] A.G. McLean et al., "Validating Divertor Power Exhaust Models with Vacuum Ultraviolet Spectroscopy in DIII-D", invited talk (JI2.00002) at the 60th annual meeting of the APS Division of Plasma Physics, Portland, Oregon, Nov 5-9, 2018.
- [23] T.D. Rognlien, et al., Contributions to Plasma Physics 34 (1994) 362.
- [24] A. Holm, et al., Nuclear Materials and Energy (2022) 101337, <https://doi.org/10.1016/j.nme.2022.101337>.